

Speckle-interferometric study of close visual binary system Hip 11253 (HD14874) using Gaia (DR2) and (EDR3)

Hussam Aljboor¹ and Ali Taani²

¹ Department of Basic Scientific Sciences, Prince Hussein Bin Abdullah II Academy for Civil Protection, Al Balqa Applied University, Amman, Jordan
Email: Hussamaljboor32@gmail.com

² Physics Department, Faculty of Science, Al Balqa Applied University, 19117 Salt, Jordan
Email: ali.taani@bau.edu.jo

ABSTRACT

We present a comprehensive set of physical and geometrical parameters for each of the components of the close visual binary system Hip 11253 (HD14874). We present an analysis for the binary and multiple stellar systems with the aim to obtain a match between the overall observational spectral energy distribution of the system and the spectral synthesis created from model atmospheres. The epoch positions are used to determine the orbital parameters and the total mass. The parameters of both components are derived as: $T_{\text{eff}}^a = 6025$, $T_{\text{eff}}^b = 4710$, $\log g_a = 4.55$, $\log g_b = 4.60$, $R_a = 1.125R_{\odot}$, $R_b = 0.88R_{\odot}$, $L_a = 1.849L_{\odot}$, $L_b = 0.342L_{\odot}$. Our analysis shows that the spectral types of both are F9a and K3b. By combining the orbital solution with the parallax measurements of Gaia DR2 and EDR3, we estimate the individual masses using H-R diagram $M_a = 1.09M_{\odot}$ and $M_b = 0.59M_{\odot}$ for using Gaia DR2 parallax and $M_a = 1.10M_{\odot}$ and $M_b = 0.61M_{\odot}$ for using Gaia EDR3 parallax. Finally, the location of both system's components on the stellar evolutionary tracks is presented.

Key word: Binaries: - close visual - stars: fundamental parameters - stars: individual (HIP11253). speckle interferometric, orbital dynamics.

1. INTRODUCTION

About half of the stars in the galaxy are binaries or stellar systems (Duquennoy & Mayor, 1991; Cai *et al.*, 2012). The analysis of binary systems is an efficient method for determining the physical and geometrical properties, such as the stellar masses. Close Visual Binary Stars (CVBSs) are binaries with a small separation angle (1 arcsecond or less) between their components, and they are hard to detect with a small telescope. Since the long orbital periods of CVBSs have a range of 10-1000 yrs., it takes a long time to observe one orbital period (Jiang *et al.*, 2013; Taani, Abushattal and Mardini 2019). The visual binaries are an important source to obtain the masses and distances of the stars, which contribute to the understanding of their basic physical properties (Taani & Vallejo 2017; Taani, Vallejo and Abu-Saleem 2022; Taani *et al.*, 2022). The recent measurements of such systems by the Gaia astrometry mission with increased precision have improved the distances to such systems (Collaboration 2018; Mardini et al. 2019a,b; Mardini et al. 2020; Brown et al. 2021). The system HIP11253 being visually close enough, enable accurate measurements of its colors, color indices, and magnitude difference between its components.

In this paper, we use two approaches. One is based on the Al-Wardat's approach (Al-Wardat 2002), which computes the entire spectral energy distribution (SED) of binary systems built with (ATALS9) atmospheric modeling (Kurucz 1994). The other approach is a dynamical estimate of the orbital parameters according to (Tokovinin 1992) based on the "ORBITX" Tokovinin's program. Details of this program can be found by (Tokovinin 2017).

A complete set of physical and orbital properties of the CVBMSs have been determined using the Tokovinin's approach (Al-Wardat and Widyan, 2009; Al-Wardat, 2012; Masda et al., 2019; Widyan and Aljboor 2021; Tawalbeh et al., 2021; Al-Wardat et al., 2021; Abu-Dhaim et al. 2022).

HIP11253 is located at a right ascension of $02^h20^m51^s$, and declination of $+30^\circ38'48''$ (SIMBAD catalog). The parallax of the system is obtained from the Gaia Data Release 2 (Collaboration 2018) and it's a value is 18.9878 ± 0.627 mas, which corresponds to a distance of 52.67pc and the Gaia Early Data Release 3 (Brown et al., 2021) and its value is 18.1854 ± 0.213 mas, which corresponds to a distance of 54.99pc. Table (1), contains the basic information on the system from the (SIMBAD) and other databases.

The aim of this study is to find reliable stellar parameters for systems that may produce the best agreement between measured magnitudes and color indices and synthetic results. In addition, we use the Gaia parallaxes DR2 (Collaboration 2018) and Gaia parallaxes EDR3 (Brown et al., 2021). We emphasize that the binary system HIP11253 is presented as an example of how to use the approach mentioned above in the case of a visual close binary of low total mass.

Properties	Parameters	Value	Reference
Position	α_{2000}	$02^h 20^m 51^s$	(SIMBAD Astronomical Database - CDS (Strasbourg), no date)
	δ_{2000}	$+30^\circ 38' 48''$	(SIMBAD Astronomical Database - CDS (Strasbourg), no date)
Magnitudes [mag]	m_v	8.16	(ESA, 1997)
	A_v	0.2432	(Schlafly and Finkbeiner, 2011)
	$(B - V)_J$	0.665 ± 0.018	(ESA, 1997)
	B_T	8.96 ± 0.012	(Hog et al., 2000)
	V_T	8.23 ± 0.010	(Hog et al., 2000)
Parallax [mas]	π_{GDR2}	18.9878 ± 0.627	(Brown et al., 2018)
	π_{GEDR3}	18.1854 ± 0.213	(Brown et al., 2021)

Table 1: Basic parameters and observed astrometric and photometric data of HIP 11253.

Δm	Tel^*	$filter(\lambda/\Delta\lambda)$	<i>Reference</i>
1.89 ± 0.03	6.0	545nm/30	(Pluzhnik, 2005)
2.79 ± 0.22	6.0	545nm/30	(Balega <i>et al.</i> , 2002)
2.48 ± 0.19	6.0	600nm/30	(Balega, Balega and Maksimov, 2006)
2.95 ± 0.00	3.5	550nm/40	(Horch <i>et al.</i> , 2008)
2.68 ± 0.05	6.0	540nm/30	(Balega <i>et al.</i> , 2007)
2.71 ± 0.00	3.5	550nm/30	(Horch <i>et al.</i> , 2009)
2.55 ± 0.00	3.5	562nm/40	(Roberts, 2011)

Table 1: Magnitude difference between the components of the system Hip11253, along with the filters used to obtain the observations.

<i>Epoch</i>	θ	$\delta\theta$	ρ	$\delta\rho$	<i>mcth</i>	<i>Reference</i>
1991.25	362	.	0.239	.	<i>Hh</i>	(Hartkopf <i>et al.</i> , 1997)
1998.7747	285.6	0.6	0.344	0.004	<i>S</i>	(Balega <i>et al.</i> , 2002)
1998.9246	285.8	.	0.347	.	<i>S</i>	(Horch <i>et al.</i> , 2002)
1999.8130	283.9	0.3	0.351	0.002	<i>S</i>	(Balega <i>et al.</i> , 2004)
2000.8730	282.7	0.5	0.356	0.003	<i>S</i>	(Balega <i>et al.</i> , 2006)
2001.7528	282.1	0.4	0.362	0.002	<i>S</i>	(Balega <i>et al.</i> , 2006)
2002.7992	278.2	1.1	0.386	0.007	<i>S</i>	(Balega <i>et al.</i> , 2013)
2003.6290	277.8	.	0.372	.	<i>S</i>	(Horch <i>et al.</i> , 2008)
2003.6290	275.7	.	0.368	.	<i>S</i>	(Horch <i>et al.</i> , 2008)

2004.8239	276.9	0.3	0.372	0.002	<i>S</i>	(Balega <i>et al.</i> , 2007)
2007.8256	273.2	.	0.379	.	<i>S</i>	(Tokovinin, Mason and Hartkopf, 2010)
2009.7371	279.7	21.7	0.350	0.05	<i>S</i>	(Voitsekhovich and Orlov, 2014)
2010.0100	269.5	.	0.373	.	<i>S</i>	(Horch <i>et al.</i> , 2011)
2012.6777	265.7	0.3	0.366	0.009	<i>S</i>	(Riddle <i>et al.</i> , 2015)
2013.7976	264.1	.	0.344	.	<i>Ag</i>	(Kehrl <i>et al.</i> , 2017)

Table 2: New data of interferometric Measurements for the HIP 11253 system.

<i>Orbital element</i>	<i>Unit</i>	<i>Last work</i> (Ling 2011)	<i>This work</i>
<i>P</i>	[<i>yr</i>]	82.18	84.48 ± 0.86
ω	[<i>deg</i>]	278.8	276.11 ± 0.27
<i>e</i>	--	0.283	0.288 ± 0.0054
Ω	[<i>deg</i>]	87.95	86.95 ± 0.16
<i>i</i>	[<i>deg</i>]	109.7	108.61 ± 0.25
<i>T</i>	[<i>yr</i>]	2026.35	2026.80 ± 0.2184
<i>a</i>	[<i>arcsec</i>]	0.378	0.3921 ± 0.008
M_T^*	[M_\odot]	1.1682	1.2342
M_T^{**}	[M_\odot]	1.3297	1.4049
<i>RMS</i> (θ)	[<i>deg</i>]	0.62	0.5907
<i>RMS</i> (ρ)	[<i>arcsec</i>]	0.0124	0.0055

Table 3: Orbital parameters solutions and total masses formerly published for the HIP 11253 system, for comparison with this work. *Using parallax Gaia Data Release 2 (DR2). ** Using parallax Gaia Data Release 3 (EDR3).

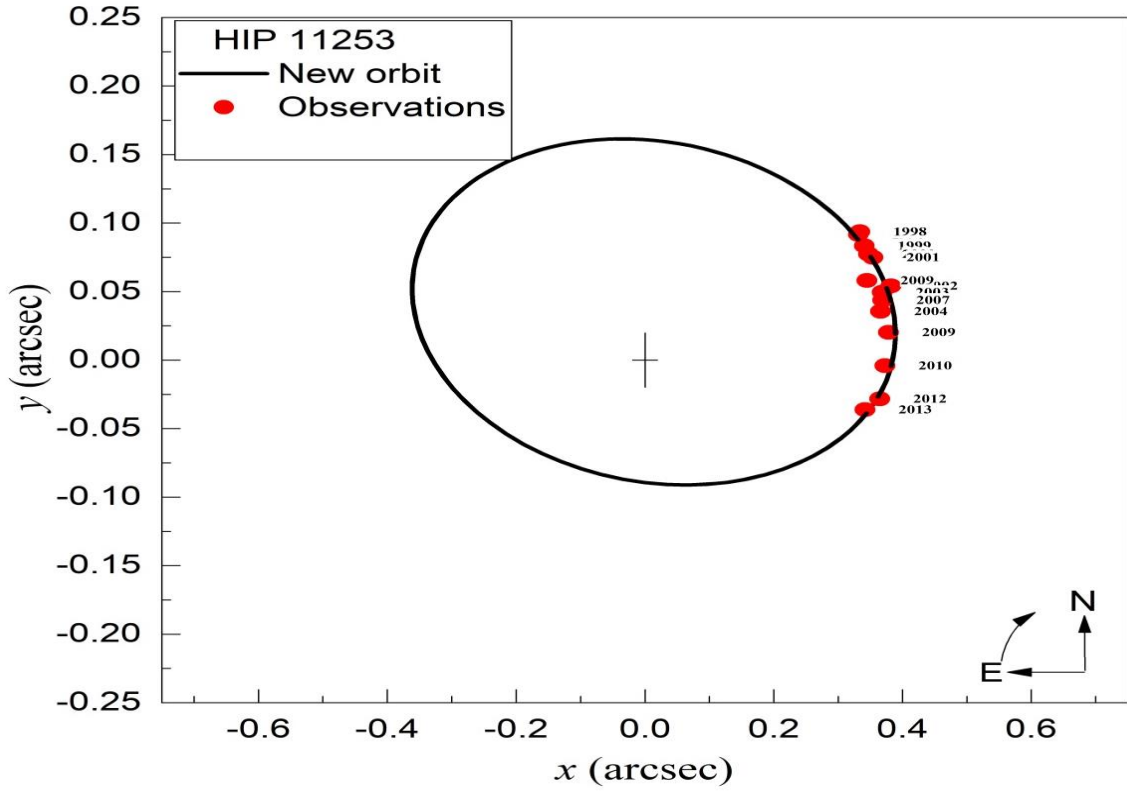


Figure 1: The relative orbit of the binary system HIP 11253 constructed using the relative position. The measurements were taken from the fourth catalog of Interferometric measurements of binary stars.

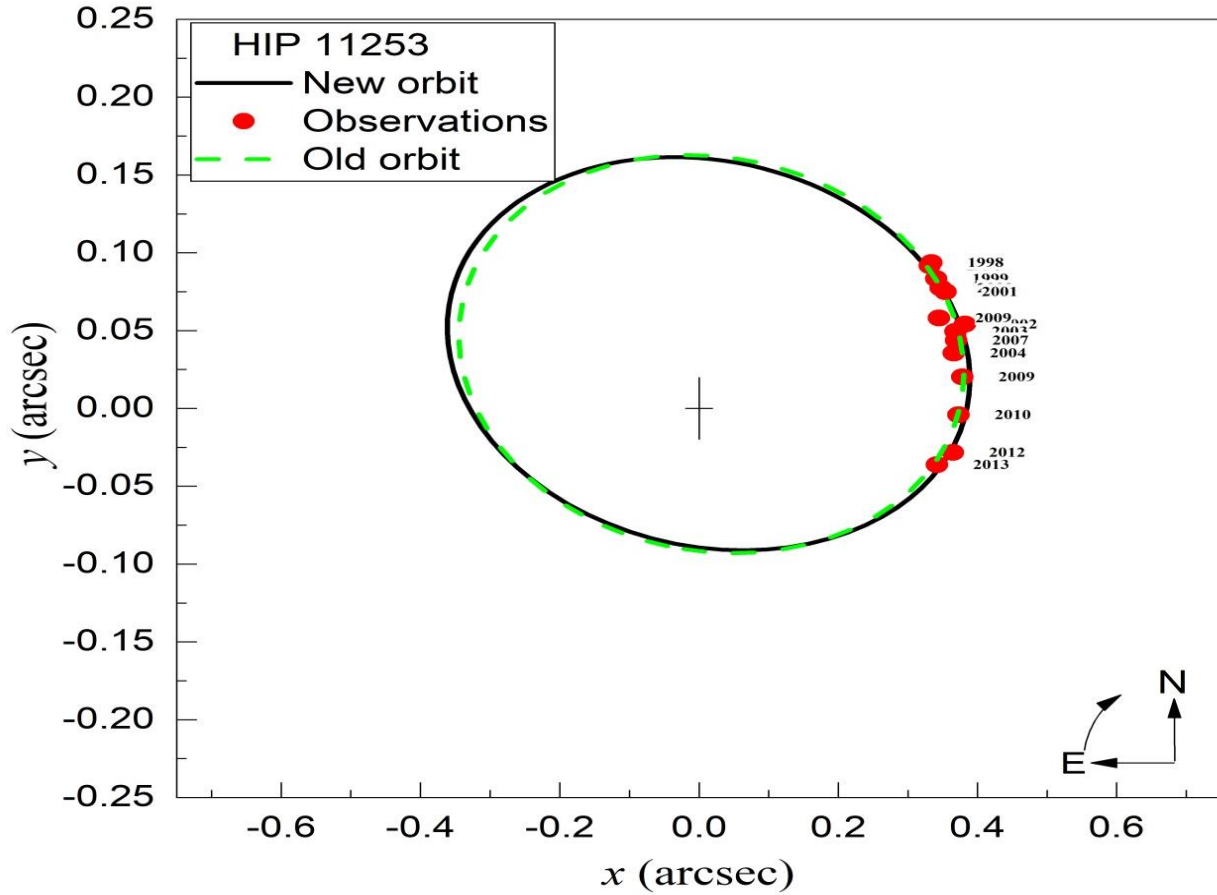


Figure 2: The different in the orbit between the last work from Ling (2011) and this work .

2. ORBTIAL ELEMENTS:

The determination of the orbital elements is crucial in calculating the stellar masses. The orbit of the HIP11253 system is obtained using the position angles (θ) and the angular separations (ρ) obtained from the fourth Catalog of Interferometric Measurement of binary stars (INT4) (see table 3), following Tokovinin's method (Tokovinin 1992). The orbit is shown in figure (1), and the results of the dynamical analysis and orbital solutions of HIP 11253 are listed in Table (4).

Table (4) shows a good agreement between our estimated orbital period (P); inclination (i); semi-major axis (a); eccentricity (e); position angle of nodes (Ω); argument of periastron (ω); and time of primary minimum (T) with those previously reported results.

Figure (2) depicts the new orbit in comparison to the old one obtained earlier by (Ling 2011). We have estimated the total dynamical mass for this binary system, using the Kepler's third law. The total dynamical mass is given by:

$$M_{\text{Dyn}} = M_A + M_B = \left(\frac{a}{\pi}\right)^3 \frac{M_{\odot}}{P^2}, \quad (2.1)$$

where a is the semi-major axis in (arcsec), π is the trigonometric parallax in (arcsec), M_A, M_B are the masses of the individual components, M_{dyn} is the dynamical mass sum, P : the relative orbital period, and M_{\odot} is the mass of the Sun equal to 1.9891×10^{30} kg.

The error of the dynamical mass sum is given by:

$$\frac{\delta_M}{M_{\text{Dyn}}} = \sqrt{9 \left(\frac{\delta_{\pi}}{\pi}\right)^2 + 9 \left(\frac{\delta_a}{a}\right)^2 + 4 \left(\frac{\delta_P}{P}\right)^2} \quad (2.2)$$

Using the orbital period and semi-major axis obtained from the orbital solution and parallax measurement, we estimate the dynamical mass as it appears in table (4).

3. ATMOSPHERIC MODELING

3.1 INPUT PARAMETERS

We derive the physical parameters of each component of the binary star system HIP11253 according to the approach by (Al-Wardat 2002). This is done by creating individual SED models for each system component using the visual magnitude $m_v = 8^m.16$ from Table (1), and the average value for visual magnitude band $\Delta m_v = 2^m.16$ from the speckle interferometric results in see Table (2), along with parallax of the system ($\pi = 18.9878, d = 52.67pc$) from Gaia DR2, ($\pi = 18.1854, d = 54.99pc$) from Gaia EDR3, and the bolometric corrections (BC) by Lang(Lang 1992). The preliminary specific value of the components input parameters

were estimated as seen in Table (5). To determine the apparent visual magnitude of individual components (m_V^A and m_V^B) we use the following equations:

$$m_V^A = m_v + 2.5 \log(1 + 10^{-0.4\Delta m_v}), \quad (3.1)$$

$$m_V^B = m_V^A + \Delta m_v \quad (3.2)$$

$$M_v = m_v + 5 + 5 \log \pi - A_v \quad (3.3)$$

Where A_v is the interstellar extinction coefficient, π the trigonometric parallax (Brown *et al.*, 2018). The absolute magnitude of individual components (M_V^A and M_V^B) can be

calculated according to the equations in Lang (1992) and Gray (2005). With the absolute

magnitude, the effective temperature (T_{eff}), and the BC can be obtained. The absolute

bolometric magnitude (M_{bol}) is then calculated using BC.

$$M_{\text{bol}} = M_V - BC \quad (3.4)$$

$$M_{\text{bol}}^* - M_{\text{bol}}^\odot = -2.5 \log \left(\frac{L^*}{L_\odot} \right). \quad (3.5)$$

Where: M_{bol}^{\odot} : is the bolometric magnitude of the Sun= $4^m.75$, L_{\odot} is Luminosity of the Sun = 3.79×10^{26} Watt, R_{\odot} is the radius of Sun = 6.957×10^5 km, T_{\odot} is the effective temperature of Sun = 5777 K, and M_{\odot} is the Mass of Sun 1.988×10^{30} kg.

The radius (R) is obtained through:

$$\log \left(\frac{R}{R_{\odot}} \right) = 0.5 \log \left(\frac{L}{L_{\odot}} \right) - 2 \log \left(\frac{T}{T_{\odot}} \right). \quad (3.6)$$

The gravitational acceleration ($\log g$) is obtained as:

$$\log g = \log \left(\frac{M}{M_{\odot}} \right) - 2 \log \left(\frac{R}{R_{\odot}} \right) + 4.43. \quad (3.7)$$

Note that the T_{eff} and $\log g$ values for both components are considered as the preliminary input parameters for both components' atmospheric modeling. As a result, we can compute their synthetic spectra.

Parameters	Unit	Gaia parallax DR2 [(Brown <i>et al.</i> , 2018)]		Gaia parallax EDR3 (Brown <i>et al.</i> , 2021)	
		A	B	A	B
m_v	[mag]	8.30	10.46	8.30	10.64
M_v	[mag]	4.45	6.61	4.36	6.52

BC*	[mag]	−0.09	−0.41	−0.08	−0.41
M _{bol}	[mag]	4.61	7.05	4.44	6.93
T _{eff} *	[k]	5987	5080	6030	4815
R	[R _☉]	2.976	1.342	3.172	1.578
L	[L _☉]	1.138	0.120	1.330	0.134
Sp – Type*	– –	G0	K2	F9	K3

Table 4: Preliminary physical and geometrical properties of HIP 11253. The properties marked by asterisks are obtained using the tables from Lang (1992) and Gray (2005).

3.2. Synthetic Spectra:

The input parameters obtained in sec. 3.1 are adopted to model the star’s atmosphere by using the blanked model (ATLAS 9) due to Kurucz’s (Kurucz 1994). As a result, the following equation is used to calculate the total synthetic SED of the binary star system as observed from the Earth, which is related to the energy flux of each component:

$$F_{\lambda} \cdot d^2 = H_{\lambda}^A \cdot R_A^2 + H_{\lambda}^B \cdot R_B^2 \quad (3.8)$$

which can be expressed as:

$$F_{\lambda} = (R_A/d)^2 [H_{\lambda}^A + H_{\lambda}^B \cdot (R_B/R_A)^2] \quad (3.9)$$

Where, $H_{\lambda}^A, H_{\lambda}^B$ are the fluxes at the surface of the star, F_{λ} is the flux for the entire (SED) of the binary system, and R_A, R_B are the radii of the primary and secondary components of the system in solar units.

Several works applied an iterative scheme using a different combination of input parameters to get the best fit between the observed flux and the total computed flux (see i.e, Al-Wardat and Widyan, 2009). Additionally, multiple values of Δm , m_v , and parallax to achieve convergence. In this way, various models are obtained and compared with the observed SED. The results are presented in the figures (3 & 4) and in Table (6).

Our criteria to find the best fit are based on the following: the inclination of the spectra,

maximum values of the fluxes, and profiles of the absorption lines. As a consequence, the best fit we have found (see figures 3 and 4) was found using the following set of parameters (see Table 6).

However, Table (7) shows the synthetic spectrum for the entire and individual components of HIP 11253. While the comparison between the observational and synthetic values for the color index and magnitude differences is listed in Table (8). A good indication of the reliability of the obtained parameters of the different system components as listed in Table (9). In addition, based on the ultimate effective temperatures of the system, we estimate the bolometric magnitudes and the stellar luminosities, by using the following equation :

$$\log \left(\frac{R}{R_{\odot}} \right) = 0.5 \log \left(\frac{L}{L_{\odot}} \right) - 2 \log \left(\frac{T}{T_{\odot}} \right). \quad (3.10)$$

$$\log g = \log \left(\frac{M}{M_{\odot}} \right) - 2 \log \left(\frac{R}{R_{\odot}} \right) + 4.43. \quad (3.11)$$

The best fit values are sufficiently representative of the system component parameters. Using Lang (1992) and Gray (2005) empirical relations of spectral types and effective temperature, the spectral types of HIP 11253 components can be obtained as (*F9*) and (*K3*) for components a and b respectively.

HIP 11253		π_{GDR2}	π_{EDR3}
Using			
Symbol	Units		
π	[<i>arcsec</i>]	18.9878	18.1854
d	[<i>pc</i>]	52.67	54.99
R_A	[R_{\odot}]	$1.125R_{\odot}$	$1.175R_{\odot}$

R_B	$[R_\odot]$	$0.88R_\odot$	$0.92R_\odot$
T_{eff}^A	$[K]$	$6025K$	$6025K$
T_{eff}^B	$[K]$	$4710K$	$4710K$
$\log g_A$	$[cm/s^2]$	4.55	4.55
$\log g_B$	$[cm/s^2]$	4.60	4.60

Table 6: The final results of this individual components and entire SEDs of the system HIP11253.

4. SYNTHETIC PHOTOMETRY

Following the treatment by Al-Wardat, (2002), the synthetic magnitudes are calculated from the synthetic SED using the following relationship:

$$m_p[F_{\lambda.s}(\lambda)] = -2.5 \log \frac{\int P_p(\lambda) F_{\lambda.s} \lambda d\lambda}{\int P_p(\lambda) F_{\lambda.r} \lambda d\lambda} + ZP_p, \quad (4.1)$$

where m_p : is the synthetic magnitude of the passband p, $P_p(\lambda)$: is the dimensionless sensitivity function of the passband p, $F_{\lambda.s}(\lambda)$: is the synthetic SED of the object, $F_{\lambda.r}(\lambda)$: is the SED of reference star Vega, ZP_p : the zero-point taken from Maíz Apellániz (2007). By using the iteration method with different sets of observed stellar parameters like magnitude differences of the components and color indices of the entire system and individual components in (U-B-V-R) Johnson-Cousins, (uvby) Strömgen and (B-V) Tycho. One can get the best fit between the observational and synthetic magnitudes. This would help us to judge the accuracy of the estimated parameters using the Interactive Data Language (IDL) program and verify the estimated parameter reliability. As we can see, figures (3) and (4) show best-fitting between the individual components and entire synthetic and observational SED. While on other hand, Figures 5 and 6, show the evolutionary tracks of in a theoretical HR diagram of the components of both HIP11253, which are evolving off the main sequence. This helped to estimate the masses and spectral types as in Table (9). Al-Wardat's approach gives a mass sum of $1.68M_\odot$ for parallax Gaia DR2 and $1.71M_\odot$ for parallax Gaia EDR3. It is worth noting that masses estimated using the Al-Wardat's approach along with the modified orbital elements is independent of the parallax value. From the comparison of dynamical masses using this

approach, we realize that parallax measurement from EDR3 provides a good indication of the mass sum, due to the advance and higher resolution.

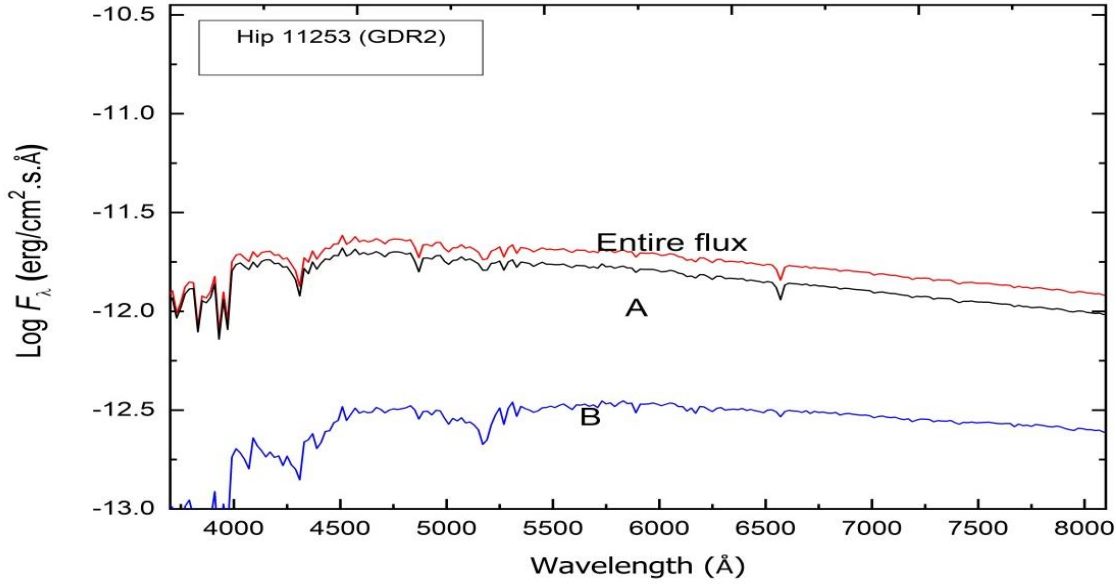


Figure3: The entire (sum of the fluxes of the members A and B) synthetic SED of the system HIP 11253 (built using parameters of the primary component, $T_{eff} = 6025k, \log g = 4.55cm/s^2, R = 1.125R_{\odot}$ and the computed flux of the secondary component with $T_{eff} = 4710k, \log g = 4.6055cm/s^2, R = 0.88R_{\odot}$ and $d = 54.99 pc$) against the observational one, the figure also shows the synthetic SED for each component

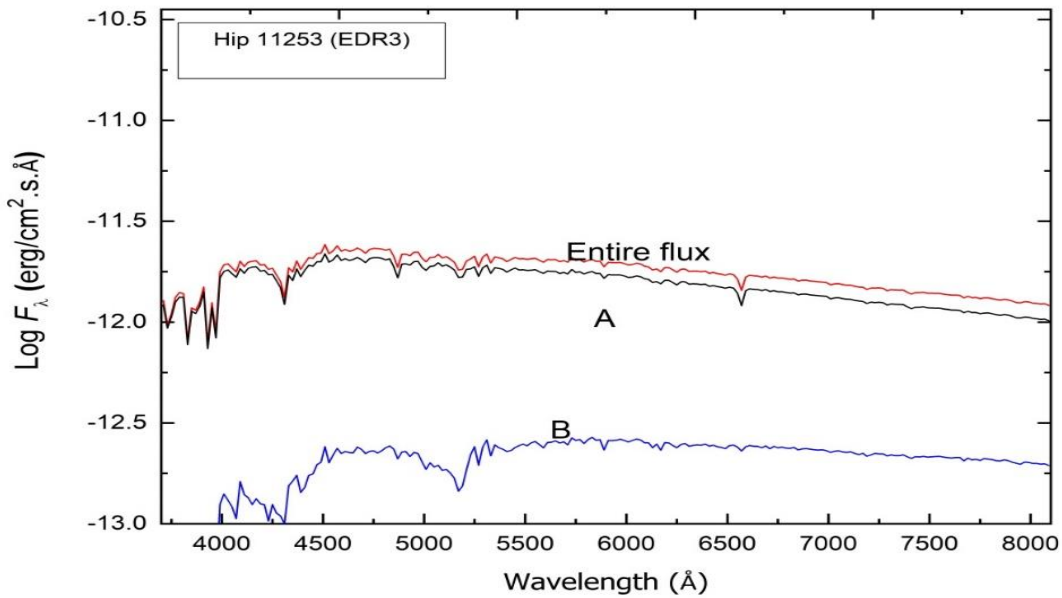


Figure 4: The entire synthetic SED of the system HIP 11253 (built using parameters of the primary component, $T_{eff} = 6025k, \log g = 4.55cm/s^2, R = 1.175R_{\odot}$ and the computed flux of the secondary component with $T_{eff} = 4710k, \log g = 4.60 \frac{cm}{s^2}, R = 092R_{\odot}$ and $d = 52.67 pc$) against the observational one ,the figure also shows the synthetic SED for each component.

Sys	Filter	HIP11253 using					
		Gaia DR2			Gaia EDR3		
		Entire Synth.	A	B	Entire Synth.	A	B
Joh-Cou.	<i>U</i>	8.9891	9.03494	12.4473	8.98816	9.03410	12.4444
	<i>B</i>	8.82499	8.91813	11.5380	8.82400	8.91726	11.5351
	<i>V</i>	<u>8.16179</u>	8.30102	10.4605	<u>8.16070</u>	8.30023	10.4576
	<i>R</i>	7.78665	7.96659	9.82692	7.78549	7.96576	9.82400
	<i>U - B</i>	0.164123	0.116807	0.99328	0.164162	0.116833	0.909332
	<i>B - V</i>	<u>0.663198</u>	0.617116	1.07748	<u>0.663301</u>	0.617037	1.07747
	<i>V - R</i>	0.375146	0.334431	0.633608	0.375205	0.334466	0.633633
Strom.	<i>u</i>	10.1379	10.1790	13.7147	10.1369	10.1781	13.7118
	<i>v</i>	9.18100	9.25202	12.1776	9.17996	9.25111	12.1748
	<i>b</i>	8.53023	8.64619	11.0157	8.52918	8.64538	11.0128
	<i>y</i>	8.12762	8.27197	10.3894	8.12655	8.27124	10.3864
	<i>u - v</i>	0.956917	0.926981	1.53713	0.956951	0.926999	1.53700
	<i>v - b</i>	0.650767	0.605830	1.16186	0.650776	0.605732	1.16202
	<i>b - y</i>	0.402607	0.374220	0.626360	0.402628	0.374146	0.626321
Tycho.	<i>B_T</i>	<u>8.98668</u>	9.06898	11.8287	<u>8.98571</u>	9.06811	11.8258
	<i>V_T</i>	<u>8.23819</u>	8.37034	10.5902	<u>8.23711</u>	8.36952	10.5873
	<i>B_T - V_T</i>	0.748486	0.698636	1.23847	0.748608	0.698564	1.23848

Table 5: Magnitudes and color indices of the entire synthetic spectrum and individual components of HIP 11253.

HIP11253			
Filter	Observed[mag]	Synthetic (This work using Gaia DR2) [mag]	Synthetic (This work using Gaia EDR3) [mag]
m_v	8.16	8.16179	8.1607
Δm	2.16	2.15948	2.15737
B_T	8.96 ± 0.012	8.98668	8.98571
V_T	8.23 ± 0.010	8.23819	8.23711
$(B - V)_J$	0.665 ± 0.018	0.663198	0.663301

Table 6: Comparison between the observational and synthetic magnitudes and colours indices for both systems. m_v : visual magnitude of the binary system hip 11253 , Δm : the speckle interferometric results in V-band , B_T : Photometric magnitude in Optical B band between 400 and 500 nm Tycho Magnitude, V_T : Photometric magnitude in optical V band between 500 and 600 nm Tycho Magnitude, $(B - V)_J$: Color index or magnitude difference between optical B band between 400 and 500 nm and Optical V band between 500 and 600 nm Johnson color index.

Component	Using Gaia DR2		Using Gaia EDR3	
	<i>A</i>	<i>B</i>	<i>A</i>	<i>B</i>
$T_{eff}(K)$	6025	4710	6025	4710
$\log g$	4.55	4.60	4.55	4.60
$Radius(R_{\odot})$	1.125	0.88	1.175	0.92
$L(L_{\odot})$	1.8486	0.3422	1.6334	0.3740
M_{bol}	4.08	5.91	4.22	5.82
M_V^*	4.16	6.39	4.30	6.30
$Sp.Type^*$	<i>F9</i>	<i>K3</i>	<i>F9</i>	<i>K3</i>
$parallax[mas]$	18.9878 ± 0.627		18.1854 ± 0.213	
$Mass, (M_{\odot})^{**}$	$M_a = 1.09M_{\odot}$ $M_b = 0.59M_{\odot}$ $M_a + M_b = 1.68M_{\odot}$		$M_a = 1.10M_{\odot}$ $M_b = 0.61M_{\odot}$ $M_a + M_b = 1.71M_{\odot}$	

Table 7: Estimated physical parameters of individual components for HIP 11253 system based on two parallax measurements. The properties marked by asterisks are obtained using the tables from Lang (1992) and Gray (2005). While the double asterisks are obtained using the tables from Girardi et al. (2000).

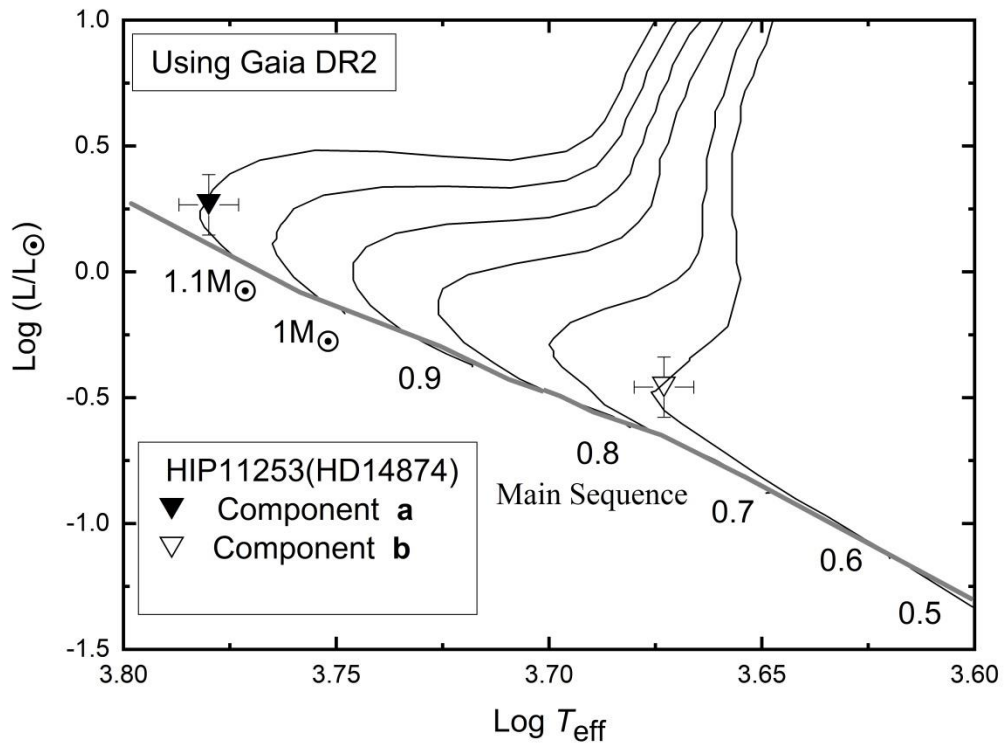


Figure 5: The evolutionary tracks of both components of HIP 11253 on the H-R diagram of masses using parallax Gaia DR2. The evolutionary tracks were taken from Girardi et al. (2000).

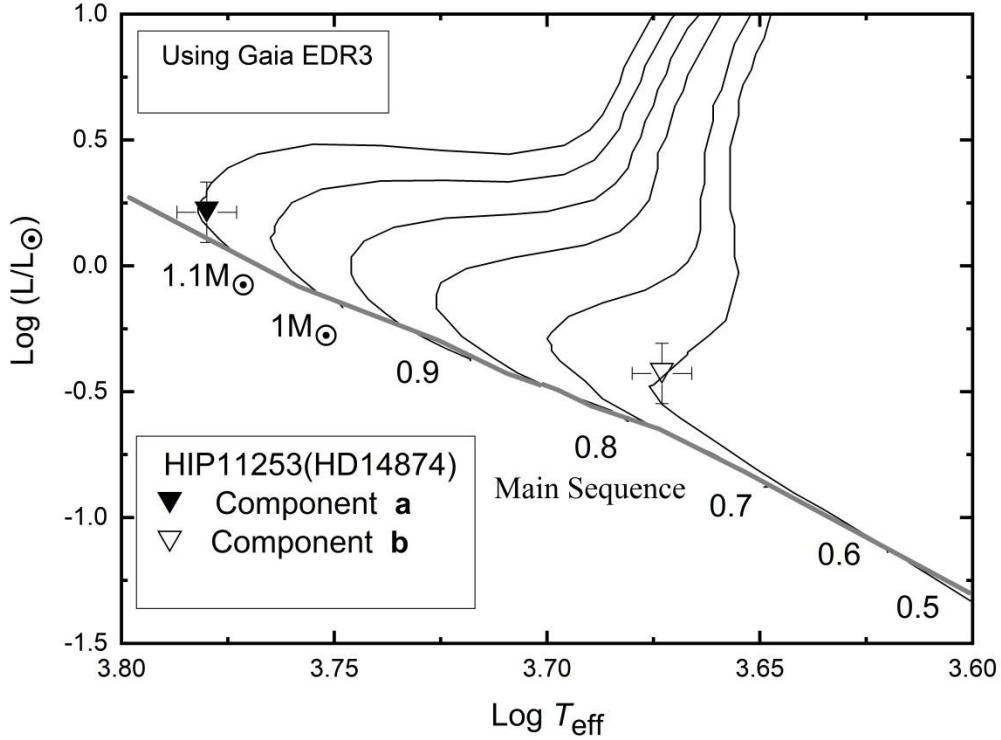


Figure 6: The evolutionary tracks of both components of HIP 11253 on the H-R diagram of masses using parallax Gaia EDR3. The evolutionart tracks were taken from Girardi et al. (2000).

5. CONCLUSIONS:

In this work, we have investigated the basic stellar parameters of the close visual binary system Hip 11253 (HD14874). Our investigation was based on the following ingredients:

- Creating individual spectral energy distribution (SED) models for each system component as described in sect. (3.1) using the approach from Al-Wardat (2002), combined with the parallax measurements by the Gaia (DR2 and EDR3).
- The orbital elements were calculated following the dynamical method used by Tokovinin (1992).
- We used the SED approach to calculate the synthetic magnitude, where the results are displayed in Figure (3) and (4).
- The spectral types of both components are identified as *F9* and *K3*, A and B respectively.

6. ACKNOWLEDGMENTS:

The authors would like to thank M. Al-Wardat for using the ORBITX code and Al-Wardat's complex method for analyzing close visual binary and multiple systems. The authors also thank Mounib Eid for providing his comments and suggestions. The authors would also like to thank the anonymous referee for the careful reading of the manuscript and for all suggestions and comments which allowed us to improve both the quality and the clarity of the paper. This work used the SAO/NASA database, Gaia Data (Gaia DR2) and (EDR3), the SIMBAD database, the fourth catalogue of interferometry measurements of binary stars. IPAC data systems and CHORIZOS code for analysis of photometric and spectrophotometric data.

7. References:

- Abu-Dhaim, A., Taani, A., Tanineah, D. \& et al. (2022) 'Studying the Physical Parameters of the Stellar Binary System Hip 42455 (HD 73900)', *Acta Astronomica* 72 (1), pp.171-181.
- Al-Tawalbeh, Y., Hussein A, Taani A., Abushattal A., \& et al. (2021) 'Precise Masses, Ages, and Orbital Parameters of the Binary Systems HIP 11352, HIP 70973, and HIP 72479', *Astrophysical Bulletin* 76 (1), pp.71-83.
- Al-Wardat, M. (2002) 'Spectrophotometry of speckle binary stars II', *Bull. Special Astrophys. Obs*, 54, pp. 29–45.
- Al-Wardat, M. A., Widyan, H., (2009), 'Parameters of the visually close binary system Hip11253 (HD14874) ' *Astrophysical Bulletin*, 64, 365-371.
- Al-Wardat, M. (2012) 'Physical Parameters of the Visually Close Binary Systems Hip70973 and Hip72479', *Publications of the Astronomical Society of Australia*, 29(4), pp. 523–528. doi:10.1071/AS12004.
- Al-Wardat, M.A., Abu-Alrob, E., Hussein, A., Mardini, M., Taani, A. (2021) 'Physical and geometrical parameters of CVBS XIV: the two nearby systems HIP 19206 and HIP 84425', *Research in Astronomy and Astrophysics*, 21, 161. 10.1088/1674-4527/21/7/161.
- Balega, I. *et al.* (2004) 'Speckle interferometry of nearby multiple stars. II.', *Astronomy & Astrophysics*, 422(2), pp. 627–629.
- Balega, I.I. *et al.* (2002) 'Speckle interferometry of nearby multiple stars', *Astronomy & Astrophysics*, 385(1), pp. 87–93.
- Balega, I.I. *et al.* (2006) 'Orbits of new Hipparcos binaries. II', *Astronomy & Astrophysics*, 448(2), pp. 703–707.
- Balega, I.I. *et al.* (2007) 'Speckle interferometry of nearby multiple stars. IV.

Measurements in 2004 and new orbits’, *Astrophysical Bulletin*, 62(4), pp. 339–351.

Balega, I.I. *et al.* (2013) ‘Speckle interferometry of nearby multiple stars. V. 2002–2006 positional measurements’, *Astrophysical Bulletin*, 68(1), pp. 53–56.

Balega, I.I., Balega, Y. u. Y. u. and Maksimov, A.F. (2006) ‘No Title’, *Bull. Spec. Astrophys. Obs.*, 59.

Brown, A.G.A. *et al.* (2018) ‘Gaia Data Release 2 Summary of the contents and survey properties’, *Astronomy & Astrophysics*, 616(1).

Brown, A.G.A. *et al.* (2021) ‘Gaia early data release 3-summary of the contents and survey properties’, *Astronomy & Astrophysics*, 649, p. A1.

Cai, Y. *et al.* (2012) ‘Statistics and evolution of pulsars’ parameters’, *Chinese Astronomy and Astrophysics*, 36(2), pp. 137–147.

Collaboration, G. (2018) ‘VizieR Online Data Catalog: Gaia DR2 (Gaia Collaboration, 2018)’, *VizieR Online Data Catalog*, pp. I–345.

Duquennoy, A. and Mayor, M. (1991) ‘Multiplicity among solar-type stars in the solar neighbourhood. II-Distribution of the orbital elements in an unbiased sample’, *Astronomy and Astrophysics*, 248, pp. 485–524.

ESA, F. (1997) ‘The Hipparcos and Tycho Catalogues’, *ESA SP*, 1200.

Gray, D.F. (2005) *The Observation and Analysis of Stellar Photospheres*.

Hartkopf, W.I. *et al.* (1997) ‘ICCD Speckle Observations of Binary Stars. XVII. Measurements During 1993-1995 From the Mount Wilson 2.5-M Telescope.’, *The Astronomical Journal*, 114, p. 1639.

Hog, E. *et al.* (2000) *The Tycho-2 catalogue of the 2.5 million brightest stars*. Naval Observatory Washington DC.

Horch, E.P. *et al.* (2002) ‘Speckle observations of binary stars with the WIYN telescope. III. A partial survey of A, F, and G dwarfs’, *The Astronomical Journal*, 124(4), p. 2245.

Horch, E.P. *et al.* (2008) ‘CHARGE-COUPLED DEVICE SPECKLE OBSERVATIONS OF BINARY STARS WITH THE WIYN* TELESCOPE. V. MEASURES DURING 2001–2006’, *The Astronomical Journal*, 136, 312.

Horch, E.P. *et al.* (2009) ‘CCD speckle observations of binary stars with the WIYN Telescope. VI. Measures during 2007–2008’, *The Astronomical Journal*, 139, 205.

Horch, E.P. *et al.* (2011) ‘Observations of binary stars with the differential

speckle survey instrument. II. Hipparcos stars observed in 2010 January and June', *The Astronomical Journal*, 141(2), p. 45.

Jiang, L. *et al.* (2013) 'Characteristic age and true age of pulsars', in *International Journal of Modern Physics: Conference Series*. World Scientific, pp. 95–98.

Kehrli, M. *et al.* (2017) 'Speckle Interferometry of Eleven Hipparcos Binary Discoveries', *Journal of Double Star Observations*, 13(1), pp. 122–130.

Kurucz, R. (1994) 'Solar abundance model atmospheres for 0,1,2,4,8 km/s.', *Solar abundance model atmospheres for 0*, 19.

Lang, K R (1992) *Astrophysical data*. New York: Springer-Verlag.

Lang, Kenneth R (1992) 'Erratum to: The Planets', in *Astrophysical Data*. Springer, p. 939.

Ling, J.F. (2011) 'First Orbit and Mass Determinations for Nine Visual Binaries', *The Astronomical Journal*, 143(1), p. 20.

Maíz Apellániz, J. (2007) 'A uniform set of optical/NIR photometric zero points to be used with CHORIZOS', in *The Future of Photometric, Spectrophotometric and Polarimetric Standardization*, p. 227.

Mardini, M. *et al.* (2019a) 'Metal-poor Stars Observed with the Automated Planet Finder Telescope. II. Chemodynamical Analysis of Six Low-metallicity Stars in the Halo System of the Milky Way', *ApJ*, 882(1), p. 27.

Mardini, M. *et al.* (2019b) 'Metal-poor stars observed with the automated planet finder telescope. I. Discovery of five carbon-enhanced metal-poor stars from LAMOST', *ApJ*, 875(2), p. 89.

Mardini, M. *et al.* (2020) 'Cosmological Insights into the Early Accretion of r-process-enhanced Stars. I. A Comprehensive Chemodynamical Analysis of LAMOST J1109+ 0754', *ApJ*, 903(2), p. 88.

Masda, S.G. *et al.* (2019) 'Physical and Dynamical Parameters of the Triple Stellar System: HIP 109951', *Astrophysical Bulletin*, 74(4), pp. 464–474. doi:10.1134/S1990341319040126.

Pluzhnik, E.A. (2005) 'Differential photometry of speckle-interferometric binary and multiple stars', *Astronomy & Astrophysics*, 431(2), pp. 587–596.

Riddle, R.L. *et al.* (2015) 'A survey of the high order multiplicity of nearby Solar-type binary stars with Robo-AO', *The Astrophysical Journal*, 799, p. 4.

Roberts, L.C. (2011) 'Astrometric and photometric measurements of binary stars with adaptive optics: Observations from 2002', *Monthly Notices of the*

Royal Astronomical Society, 413(2), pp. 1200–1205. doi:10.1111/j.1365-2966.2011.18205.x.

Schlafly, E.F. and Finkbeiner, D.P. (2011) ‘MEASURING REDDENING WITH SLOAN DIGITAL SKY SURVEY STELLAR SPECTRA AND RECALIBRATING SFD’, *The Astrophysical Journal*, 737(2), p. 103. doi:10.1088/0004-637X/737/2/103.

SIMBAD Astronomical Database - CDS (Strasbourg) (no date). Available at: <http://simbad.u-strasbg.fr/simbad/> (Accessed: 28 April 2022).

Taani, A. and Vallejo, J. C. (2017) ‘Dynamical Monte Carlo simulations of 3-D galactic systems in axisymmetric and triaxial potentials’, *Publications of the Astronomical Society of Australia*, 34, E024. doi:10.1017/pasa.2017.17.

Taani, A., Abushattal, A. and Mardini, M.K. (2019) ‘The regular dynamics through the finite-time Lyapunov exponent distributions in 3D Hamiltonian systems’, *Astronomische Nachrichten*, 340(9–10), pp. 847–851.

Taani, A. *et al.* (2022) ‘Determination of wind-fed model parameters of neutron stars in high-mass X-ray binaries’, *Publications of the Astronomical Society of Australia*, 39, p. e040.

Taani, A., Vallejo, J.C. and Abu-Saleem, M. (2022) ‘Assessing the complexity of orbital parameters after asymmetric kick in binary pulsars’, *Journal of High Energy Astrophysics*, 35, pp. 83–90.

Tokovinin, A. (1992) ‘Astronomical Society of the Pacific Conference Series’, in *IAU Colloq. 135: Complementary Approaches to Double and Multiple Star Research*, p. 573.

Tokovinin, A. (2017) ‘New Orbits Based on Speckle Interferometry at SOAR. II.’, *The Astronomical Journal*, 154(3), p. 110.

Tokovinin, A., Mason, B.D. and Hartkopf, W.I. (2010) ‘Speckle Interferometry at the Blanco and SOAR Telescopes in 2008 and 2009’, *The Astronomical Journal*, 139(2), p. 743.

Voitsekhovich, V. V. and Orlov, V.G. (2014) ‘Temporal properties of the brightest speckle’, *Revista Mexicana de Astronomia y Astrofisica*, 50(1), pp. 37–40.

Widyan, H. and Aljboor, H. (2021) ‘Physical and orbital properties of the stellar system HIP 43766’, *Research in Astronomy and Astrophysics*, 21(5), p. 110.

